Roles of the Donor and Acceptor Chains in the Metal-Insulator Transition in TTF-TCNQ (Tetrathiafulvalene Tetracyanoquinodimethane)

Yaffa Tomkiewicz, A. R. Taranko, and J. B. Torrance
IBM Thomas J. Watson Research Center, Yorktown Heights, New York 10598
(Received 18 June 1975; revised manuscript received 30 December 1975)

The separate contributions of the TTF and TCNQ chains to the total magnetic susceptibility of TTF-TCNQ are evaluated from measurements of the gyromagnetic ratio and EPR linewidth. From the temperature dependence of these susceptibilities, we show that the metal-insulator transition at 54°K affects primarily the TCNQ chain. The TTF chain is primarily affected by the transition at 38°K and dominates the conductivity in the semiconducting regime.

The electronic properties of TTF-TCNQ have been described[1] in terms of two partially filled bands corresponding to the donor and the acceptor chains. Each of these bands makes a contribution to the measured physical properties such as conductivity[2,3] and susceptibility.[4-6] In general, the role of each chain in determining the magnitude of a given property is difficult to delineate because the respective contribution of the donor or acceptor stack is modified by the presence of the other. The only known exceptions are the gyromagnetic ratios of the TTF and TCNQ chains which were shown[7] to maintain their intrinsic g values in TTF-TCNQ. Moreover these g values are very different,[8,9] since the TTF molecule has a much bigger[10] spin-orbit coupling than TCNQ.

In the present paper we shall show how the magnetic susceptibility can be separated into TTF and TCNQ contributions using EPR g values[11] and linewidth measurements. The temperature dependence of the individual susceptibilities in the temperature range which includes both the 54 and 38°K phase transitions is used to evaluate the respective effects of these transitions on the donor and acceptor chains. The 54°K transition is shown to affect primarily the TCNQ chain, while the TTF chain is primarily affected by the 38°K transition. The separation of the susceptibility for $20°K < T < 54°K$ into its components is accomplished by using the g value of the single EPR absorption line observed. As an example of the strong temperature dependence of g for $T < 80°K$, data for $\vec{H}_{dc} \parallel \vec{c}^*$ are shown in Fig. 1. As was shown previously,[4] the isotropic part of the g value in the 25–38°K region is the same as the isotropic part of the g value obtained[12] in $(TTF)Cl_{0.8}$ and the g value[8] of the $(TTF)^+$ cation in solution. This fact, combined with the activated nature of the susceptibility,[4-6] clearly indicates that the measured susceptibility in this temperature region is all on the TTF stack, presumably because the magnetic gap on the TCNQ stack is greater than the magnetic gap on TTF. Similar behavior[13] was observed in TMTTF-TCNQ (TMTTF is tetramethyl-TTF) and also[14] for some compositions of the isostructural series $(TSeF)_x(TTF)_{1-x}$-(TCNQ) (TSeF is tetraselenafulvalene),[15] where $0 \leq x \leq 1$. However the magnetic gap on the acceptor chain depends on the nature of those chains. For example, the reported[16] g values for TTF-TNAP (TNAP is 11,11,12,12-tetracyanonaphtho-2,6-quinodimethane) indicate that the magnetic gap in the semiconducting regime is smaller on the *acceptor* chain than on the donor chain. The separate donor and acceptor contributions to the total susceptibility can be quantitatively determined in these systems using the method developed in this paper for TTF-TCNQ.

The Lorentzian shape of the single EPR absorption line strongly suggests[10] that the magnetic excitations on both stacks are coherently mixed and therefore can be treated within the strong-coupling approximation. The g value measured at a given angle θ is then related to the g values of the TTF $[g_F(\theta)]$ and TCNQ $[g_Q(\theta)]$ stacks by[10]

$$g(T,\theta) = \alpha(T) g_Q(\theta) + [1 - \alpha(T)] g_F(\theta), \qquad (1)$$

where $\alpha(T)$ is the fraction of the susceptibility on

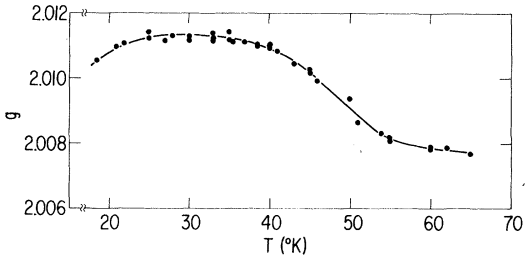

FIG. 1. Temperature dependence of g for $\vec{H}_{dc} \parallel \vec{c}^*$.

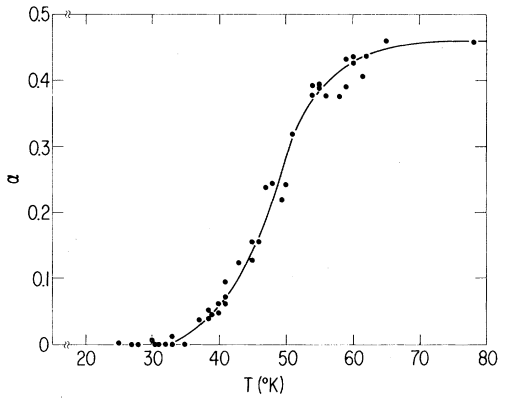

FIG. 2. Temperature dependence of α obtained from g values.

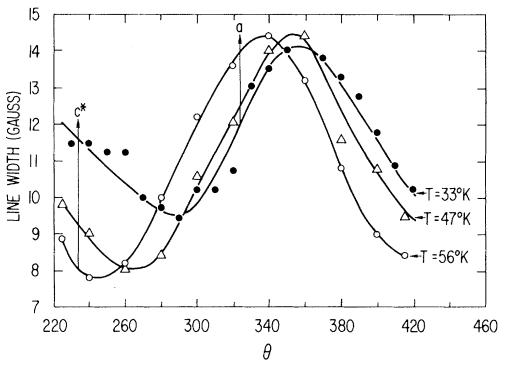

FIG. 3. Normalized linewidth anisotropy in a-c^* plane for three different temperatures. The normalization factors for the 47 and 33°K curves are 1.95 and 10.3, respectively.

the TCNQ stack,

$$\alpha(T)=\chi_Q(T)/[\chi_Q(T)+\chi_F(T)]. \quad (2)$$

The values of $g_F(\theta)$ are known[4,7] from g anisotropy measurements in the 25–35°K range, where the magnetic excitations are solely on the TTF chain. For $g_Q(\theta)$, we have chosen experimental values obtained[13] from measurements on NMP-TCNQ (NNP is N-methylphenazinium) for similar orientations of the TCNQ molecule. For example, for $\vec{H}_{dc}\parallel\vec{c}^*$ we use $g=2.0032$. Evaluation of $\alpha(T)$ using the experimentally measured g values (e.g., Fig. 1) and Eq. (1) yields the temperature dependence shown in Fig. 2.

As a further check on the consistency of this picture, we can independently determine α from linewidth considerations. The measured linewidth is represented in the strong-coupling limit by[10]

$$\frac{1}{T_2(T)}=\frac{\alpha(T)}{T_{2,Q}(T)}+\frac{1-\alpha(T)}{T_{2,F}(T)}, \quad (3)$$

where $1/T_{2,Q}$ and $1/T_{2,F}$ are the intrinsic linewidths on the TCNQ and TTF stacks. Equation (3) implies that the *anisotropy* of the measured linewidth will be temperature dependent [because of $\alpha(T)$] if the intrinsic linewidths on the individual chains have different anisotropies. The three curves in Fig. 3 represent the linewidth anisotropy in the a-c^* plane measured at 56, 47, and 33°K. The linewidth anisotropy seems to change with temperature in the same range of temperature as the g values. In general, evaluation of α from linewidth anisotropy is much more complicated than its evaluation from g values, since the intrinsic linewidths of the chains are temperature dependent. However, the linewidth anisotropy of the TTF chain (the curve corresponding to 33°K, Fig. 3) provides a clue for the determination of α. The measured linewidths in the a and c^* directions, $1/T_{2,F}(a)$ and $1/T_{2,F}(c^*)$, are observed to be approximately equal and therefore

$$\frac{1}{T_2(a)}-\frac{1}{T_2(c^*)}=\left(\frac{1}{T_{2,Q}(a)}-\frac{1}{T_{2,Q}(c^*)}\right)\alpha(T). \quad (4)$$

If the linewidth anisotropy on the TCNQ stack for $\vec{H}_{dc}\parallel\vec{a}$ and $\vec{H}_{dc}\parallel\vec{c}^*$ orientations is temperature independent, one can obtain $\alpha(T)$ (in arbitrary units). The temperature dependence of α obtained in this way agrees reasonably well with that evaluated from g values (Fig. 2).

Using Eq. (2) and the values of $\alpha(T)$ appearing in Fig. 2, one can separate the experimental magnetic susceptibility[17] into TTF and TCNQ contributions as shown in Fig. 4. No decomposition of the susceptibility was performed for $T<20$°K because of the presently not understood temperature dependence of g in this temperature region (Fig. 1).

It is clearly seen from Fig. 4 that the behaviors of the two susceptibilities are considerably different. For example, the metal-insulator phase transition at 54°K gives rise to a sudden decrease in the susceptibility on the TCNQ stack, while the TTF susceptibility appears to be only weakly affected. This observation clearly indicates that the 54°K Peierls[18] transition most strongly involves[19] the TCNQ stack. The role of the TTF stack is less clear, but appears to be more involved with the second phase transition[20] which occurs near 38°K, as judged by the fact that the TTF susceptibility starts decreasing near this temperature.

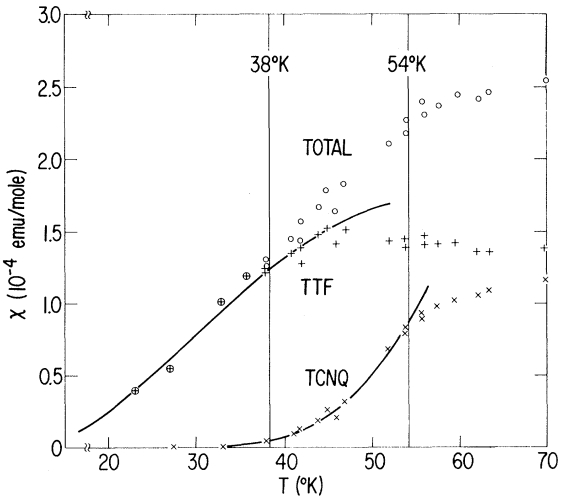

FIG. 4. The susceptibilities of the individual chains and the total measured susceptibility. The full lines correspond to the calculated values obtained from activation energies $\Delta_F = 94$°K and $\Delta_Q = 400$°K.

A quantitative measure of the rate of the decrease of the susceptibilities was obtained by an empirical fit of the form

$$T\chi(T) = c \exp(-\Delta/T). \quad (5)$$

The fits shown in Fig. 4 by solid lines are for $\Delta_Q = 400$°K and $\Delta_F = 94$°K for the TCNQ and TTF susceptibilities, respectively. The physical meaning of this fit might be that the gaps over the measured temperature regime either are temperature independent or have a linear temperature dependence. However the values of the parameters Δ_Q and Δ_F should be treated with some reservation[21] because of the narrow temperature range of the fits, the scatter of the data, and insufficient data below 38°K. The higher activation energy found for the TCNQ is consistent with (1) the previous conclusion that this chain is primarily involved with the 54°K transition and (2) the larger bandwidth calculated[22] for the TCNQ chain. Nevertheless, it is interesting to point out that the value for Δ_Q compares well with the infrared gap of 1000°K assigned[23] to the TCNQ stack and implies[24,25] a mean-field transition temperature of about 250°K. We note that the conclusion that the TCNQ stack drives the Peierls transition might seem contradictory with the previously presented[4] view that this stack is an insulator. In the previous view, the TCNQ stack was identified as the nonconducting stack on the basis of the extreme narrowness and unusual temperature dependence of the observed EPR linewidth and the unusual temperature dependence of the susceptibility. However, these features can also be explained[15,26] by the quasi-one-dimensional nature of the stacks together with the assumption that at least one of these stacks has a mean-field transition temperature in the vicinity of room temperature. The latter explanation is consistent with the present results if the stack with the high mean-field transition temperature is taken to be the TCNQ stack. How this particular feature of TCNQ affects its contribution to the conductivity is still a subject of active controversy.[27,28]

Some information about the respective contributions of the TTF and TCNQ stacks to the conductivity, σ, can be obtained by comparing $\sigma(T)$ with $\chi_F(T)$ and $\chi_Q(T)$. For example, between 54 and 38°K σ falls exponentially,[29] while χ_F is almost temperature independent. There are two possible explanations for this behavior: (1) $\sigma_F \ll \sigma_Q$ in this region and hence $\sigma(T)$ is dominated by σ_Q; or (2) σ_F and χ_F are not coupled, so that σ_F can decrease exponentially, while χ_F is constant. According to the first possibility, $\sigma \approx \sigma_Q$, which can then be compared to χ_Q. Below 51°K both σ and $\chi_Q T$ decrease exponentially with decreasing temperature, with activation energies of 250°K[20,29] and 400°K, respectively. However, one would expect the conductivity to decrease *as fast* or *faster* than the susceptibility because any electron that can conduct can flip its spin but not vice versa. Therefore, the second possibility must be true, namely the conductivity is dominated by the TTF stack[30] and the conductivity and susceptibility are decoupled. This behavior might be caused by appreciable[31] electron correlation or by an activated mobility on the TTF stack. Further work on this subject is in progress.

In conclusion, we have shown that (1) the metal-insulator transition at 54°K affects primarily the TCNQ stacks; (2) the TTF stacks are more involved in the transition at 38°K; and (3) the conductivity below 54°K is dominated by the TTF stack. The authors gratefully acknowledge helpful discussions with T. D. Schultz, B. D. Silverman, R. A. Craven, and A. J. Berlinsky. TTF-TCNQ crystals provided by E. M. Engler and susceptibility data provided by J. C. Scott are greatly appreciated.

[1]See, for example, M. H. Cohen, J. A. Hertz, P. M. Horn, and V. K. S. Shante, Bull. Am. Phys. Soc. 19,

297 (1974); A. N. Bloch, in *Energy and Charge Transfer in Organic Semiconductors*, edited by K. Masuda and M. Silver (Plenum, New York, 1974), p. 159; U. Bernstein, P. M. Chaikin, and P. Pincus, Phys. Rev. Lett. 34, 271 (1975).

[2]J. Ferraris, D. O. Cowan, V. Walatka, and J. H. Perlstein, J. Am. Chem. Soc. 95, 948 (1973).

[3]L. B. Coleman, M. J. Cohen, D. J. Sandman, F. G. Yamagashi, A. F. Garito, and A. J. Heeger, Solid State Commun. 12, 1125 (1973).

[4]Yaffa Tomkiewicz, B. A. Scott, L. J. Tao, and R. S. Title, Phys. Rev. Lett. 32, 1363 (1974).

[5]J. C. Scott, A. F. Garito, and A. J. Heeger, Phys. Rev. B 10, 3131 (1974).

[6]J. E. Gulley and J. F. Weiher, Phys. Rev. Lett. 34, 1061 (1975).

[7]W. M. Walsh, Jr., L. W. Rupp, Jr., D. E. Schafer, and G. A. Thomas, Bull. Am. Phys. Soc. 19, 296 (1974).

[8]F. Wudl, G. M. Smith, and E. J. Hufnagel, J. Chem. Soc. D 1970, 1453.

[9]M. Kinoshita and H. Akamatu, Nature (London) 207, 291 (1965).

[10]A. Carrington and A. D. McLachlan, *Introduction to Magnetic Resonance* (Harper and Row, New York, 1966).

[11]A similar approach was suggested independently by A. J. Berlinsky and J. F. Carolan.

[12]Yaffa Tomkiewicz, F. Mehran, D. C. Green, and B. A. Scott, Bull. Am Phys. Soc 19, 334 (1974).

[13]Yaffa Tomkiewicz, unpublished.

[14]Yaffa Tomkiewicz and E. M. Engler, to be published.

[15]Yaffa Tomkiewicz, E. M. Engler, and T. D. Schultz, Phys. Rev. Lett. 35, 456 (1975).

[16]P. A. Berger, D. J. Dahm, G. R. Johnson, M. G. Miles, and J. D. Wilson, Phys. Rev. B 12, 4085 (1975).

[17]The total susceptibility data appearing in this report are the data published in Ref. 5, and were kindly provided to us by J. C. Scott. We preferred these data to ours because the susceptibility tail, indicating the presence of impurities or imperfections, was absent.

[18]F. Denoyer, R. Comès, A. F. Garito, and A. J. Heeger, Phys. Rev. Lett. 35, 445 (1975).

[19]Using different arguments, T. D. Schultz and S. Etemad (to be published) have come to the same conclusion.

[20]S. Etemad, Phys. Rev. B (to be published).

[21]More detailed analysis should be possible with single-crystal measurements of (1) static susceptibility by R. M. Herman, R. A. Craven, and M. B. Salamon, to be published; and of (2) EPR susceptibility by Y. Tomkiewicz, A. R. Taranko, and J. B. Torrance, to be published.

[22]A. J. Berlinsky, J. F. Carolan, and L. Weiler, Solid State Commun. 15, 195 (1974).

[23]D. B. Tanner, C. S. Jacobsen, A. F. Garito, and A. J. Heeger, Phys. Rev. Lett. 32, 1301 (1974).

[24]M. J. Rice and S. Strassler, Solid State Commun. 13, 125 (1973).

[25]P. A. Lee, T. M. Rice, and P. W. Anderson, Phys. Rev. Lett. 31, 462 (1973).

[26]Y. Tomkiewicz, T. D. Schultz, E. M. Engler, A. R. Taranko, and A. N. Bloch, Bull. Am. Phys. Soc. 29, 287 (1976).

[27]H. Fukuyama, T. M. Rice, and C. M. Varma, Phys. Rev. Lett. 33, 305 (1974).

[28]B. R. Patton and L. J. Sham, Phys. Rev. Lett. 33, 638 (1974).

[29]P. M. Horn and D. S. Rimai, to be published.

[30]Similar conclusions were reached by Etemad (Ref.20) and P. M. Chaikin, R. L. Greene, S. Etemad, and E. M. Engler, Phys. Rev. B 13, 1627 (1976).

[31]J. B. Torrance, B. A. Scott, and F. B. Kaufman, Solid State Commun. 17, 1369 (1975).

Neural Counting and Photon Counting in the Presence of Dead Time*

Malvin Carl Teich† and William J. McGill
Columbia University, New York, New York 10027
(Received 10 November 1975)

The usual stimulus-based neural counting model for audition is found to be mathematically identical to the well-known semiclassical formalism for photon counting. In particular, we explicitly demonstrate the equivalence of McGill's noncentral negative binomial distribution and Peřina's multimode confluent hypergeometric distribution for a coherent signal imbedded in chaotic noise. Dead-time corrections, important both in neural counting and in photon counting, are incorporated in a generalized form of this distribution. Some specific implications of these results are discussed.

In an attempt to explain the relative frequency of multiple occurrences of accidents in a factory population, Greenwood and Yule[1] in 1920 provided an important and remarkably simple generalization of the Poisson process. These authors assumed that although the probability of accident for a given worker follows the simple Poisson law, variation in individual proneness to accident causes the accident rate to vary from individual to individual in the population. They then calculated the overall probability of multiple accidents using certain plausible density functions for this